6th annual IEEE Conference on Automation Science and Engineering
Marriott Eaton Centre Hotel
Toronto, Ontario, Canada, August 21-24, 2010

Directed Motion of an Atomic Scale Engine and Stability Analysis

Yi Guo*, Wenlin Zhang and Zheng Wang

***Abstract*— Atomic scale engines have received increasing research interests due to recent advances in nano-particle manipulation techniques. We study the model of an artificial atomic scale engine proposed by [1], and show numerically that the model exhibits directed motion under asymmetric particle coupling. We then conduct stability analysis of a 3-particle engine and prove that stable and unstable equilibrium points arise in an alternating sequence thus step motion can be deduced. Our analytic understanding of the complex nonlinear dynamics may guide future design of such an envisioned engine at the atomic scale.**

I. Introduction

Since the significant advances in experimental techniques in nanoscale characteristics and manipulation, there has been a growing interest in atomic scale engines during the past two decades. Among molecule transportation devices, the ratchet systems introduced in Feynman's Lectures of Physics [2] consists of a ratchet with asymmetric "teeth" and a pawl which allows the shaft to turn only one way. The mechanism could transform the incidental oscillations of the vane into a uniform circular motion of the ratchet and pawl. Theoretical aspects of the ratchet system were discussed in many references including [3], [4]. The molecule motor and biological motors discussed in [5], [6], [7], [8], [9], [10] are inspired by the behaviors in the biological realm where chemical energy is converted into mechanical energy. More recently, a primitive nanovehicle that rolls on a surface is developed in [11], [12], which converts energy-inputs from heat or electrical fields into controlled motion and transports nanocargo on the surface. Suo and his group [13], [14] demonstrated that molecules placed on a dielectric substrate surface can be programmed for patterning and can move in a desired trajectory, which uses the principle that a nonuniform electric field can direct the motion of the molecule. Suo also envisions a molecule highway in a MIT seminar that uses chemical gradient to drive the car in each track and uses electrodes to switch the car from one track to another [15]. Although some of the ideas in this area are not implementable immediately, theoretical research along this direction will provide guidances for future engine design at this scale.

A model based on one-dimensional particles sliding on a surface was proposed in [16], [1], [17], and its basic principles of functioning was explained therein as that the dynamic competition between the intrinsic lengths of the moving object and the supporting carrier is transformed to directed motion. The model is based on computer simulations without rigorous theoretical justification and experimental support. It was later reported that the concept works at different scale levels experimentally [18]. It is possible to implement it by manipulation of the motion of molecules, nanoparticles on profiled solid surfaces with periodic perturbations of the desired frequency and amplitude [18].

*Corresponding author. Ph: (201) 216 5658. Fax: (201) 216 8246.
The authors are with the Department of Electrical and Computer Engineering, Stevens Institute of Technology, Hoboken, NJ 07030. {yi.guo,zheng.wang,wzhang5}@stevens.edu

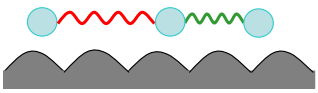

Fig. 1. A general model of coupled particles on a surface.

In this paper, we study the stability property of the engine model that was proposed in [1]. This explains the step motion of the engine analytically, and provides theoretically the possible locations where the engine stops. The model presents a nonlinear interconnected system, we study local stability of the equilibrium points using matrix and linear system theory. Existing results on the model are limited in numerical simulations and there is no analytic understanding of the complex dynamic behavior of the model. Our results explains the nonlinear dynamics analytically using control theoretical methods, which may guide the design of such a nanoscale engine in the future. Our analytic results are verified by Matlab simulations.

The rest of the paper is organized as follows. We first present in Section II the general model of the atomic scale engine, and numerical simulation results are shown for different engine capabilities including step motion, continuous moving, and cargo load carrying. We then conduct analytic stability analysis for a typical three-particle engine in Section III, and control theoretical results are presented to explain the step motion of the engine. Simulation results are also shown to support the stability claim. We will finally conclude in Section IV.

II. Model of Atomic Scale Engine and Directed Motion

We consider a model of a chain of N identical particles moving on an isotropic surface [1]. Each particle i has a mass m and is located at coordinate ϕ_i. We restrict of the translational motion in one-dimension. Fig. 1 shows the model for $N = 3$. The basic equation of motion is derived from the Newton's laws of motion

$$m\ddot{\phi}_i + \eta\dot{\phi}_i + \frac{\partial U(\phi_i)}{\partial \phi_i} + \sum_{j=i\pm 1} \frac{\partial W(\phi_i - \phi_j)}{\partial \phi_j} = 0, \quad (1)$$

978-1-4244-5449-5/10/$26.00 ©2010 IEEE

where $i = 1, \ldots, N$, $U(x_i)$ and $W(x_i - x_j)$ are the periodic potential applied by the substrate and the inter-particle interaction potential, respectively, γ is the positive linear friction coefficient.

We assume that the substrate and inter-particle potentials take the following form:

$$U(\phi_i) = -\Phi_0 \cos(\frac{2\pi\phi_i}{b}) \tag{2}$$

$$W(\phi_i - \phi_{i+\delta_i}) = \frac{k}{2}[|\phi_i - \phi_{i+\delta_i}| - A_{i+\delta_i}(t)]^2 \tag{3}$$

where $\delta_i = \pm 1$ denoting the nearest neighboring particles,

$$A_{i+\delta_i}(t) = a[1 + \alpha(qB_{i+\delta_i} + \omega t)] \tag{4}$$

$$B_{i+\delta_i} = \begin{cases} (i-1)b & \text{if } \delta_i = -1, \\ ib & \text{if } \delta_i = 1, \end{cases}$$

$$\alpha(s) = \begin{cases} c\sin(\pi s/s_0) & \text{for } 0 \le s \le s_0 \\ 0 & \text{else} \end{cases} \tag{5}$$

and k, a, c, s_0 are positive intrinsic parameters, q and ω are the wavelength and frequency of external excitation, respectively, and b is a positive constant denoting the step length.

It was first demonstrated in [1] that the system (1) exhibits directed motion under asymmetric particle coupling, that is, $A_{i+1} \neq A_{i-1}$. In the following, we show numerical simulations of different types of directed motion of the system (1).

A. Step Motion of a 3-Particle Chain

Taking $N = 3$, denoting the state as $x_{i1} = \phi_i, x_{i2} = \dot{\phi}_i$, we have the state-space representation as

$$\begin{aligned}
\dot{x}_{11} &= x_{12} \\
\dot{x}_{12} &= -(1/m)\{\eta x_{12} + \frac{2\pi}{b}\Phi_0 \sin(2\pi x_{11}/b) \\
&\quad -k[|x_{21} - x_{11}| - a(1 + \alpha(qb + \omega t))]\} \\
\dot{x}_{21} &= x_{22} \\
\dot{x}_{22} &= -(1/m)\{\eta x_{22} + \frac{2\pi}{b}\Phi_0 \sin(2\pi x_{21}/b) \\
&\quad +k[|x_{21} - x_{11}| - a(1 + \alpha(qb + \omega t))] \\
&\quad -k[|x_{31} - x_{21}| - a(1 + \alpha(2qb + \omega t))]\} \\
\dot{x}_{31} &= x_{32} \\
\dot{x}_{32} &= -(1/m)\{\eta x_{32} + \frac{2\pi}{b}\Phi_0 \sin(2\pi x_{31}/b) \\
&\quad +k[|x_{31} - x_{21}| - a(1 + \alpha(2qb + \omega t))]\}
\end{aligned} \tag{6}$$

If we choose the parameters as [1]

$$\begin{aligned}
&b = 1, \quad m = 1, \quad \Phi_0 = 1, \quad , \eta = \frac{16\pi}{10b}\sqrt{\Phi_0 m}, \\
&\omega = \frac{\pi}{25b}\sqrt{\frac{\Phi_0}{m}}, \quad k = \left(\frac{2\pi}{b}\right)^2 \Phi_0, \\
&c = \frac{7}{10}, \quad s_0 = \frac{4}{10}, \quad a = \frac{11}{10}b, \quad q = \frac{1}{5}b,
\end{aligned} \tag{7}$$

we have a step motion of the particle chain as shown in Fig. 2.

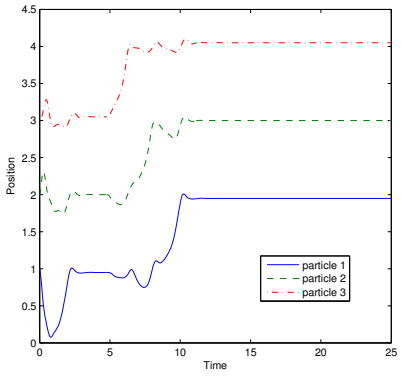

Fig. 2. Step motion of a three-particle engine.

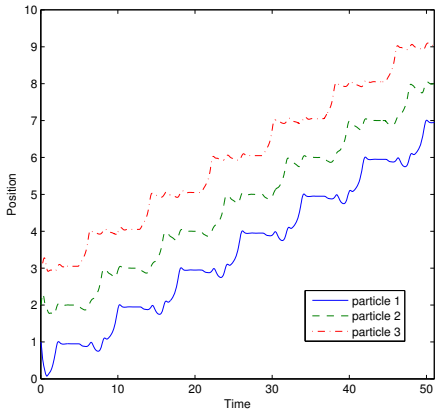

Fig. 3. Continuous motion of a three-particle motion.

B. Continuous Motion

If we change the function $\alpha(s)$ as in (5) to be periodical

$$\alpha(s) = \begin{cases} c\sin(\pi(s-l)/s_0) & \text{for } 0 \le (s-l) \le s_0 \\ 0 & \text{for } s_0 \le (s-l) \le 1 \end{cases} \tag{8}$$

where $l = 0, 1, 2, \ldots$, the particle chain has a continuous motion with an almost-constant velocity, which is shown in Fig. 3.

C. Directed Motion with Cargo Load

The atomic scale engine model shown above is capable of carrying cargo load. We add 3 cargo particles after a 6-particle engine system, with a constant rest-length interactions between cargo particles and between the cargo and the engine. The state space model is written as

$$\dot{x}_{11} = x_{12} \tag{9}$$

$$\begin{aligned}
\dot{x}_{12} &= -(1/m)\{\eta x_{12} + \frac{2\pi}{b}\Phi_0 \sin(2\pi x_{11}/b) \\
&\quad -k(|x_{21} - x_{11}| - a)\}
\end{aligned} \tag{10}$$

$$\dot{x}_{21} = x_{22} \tag{11}$$

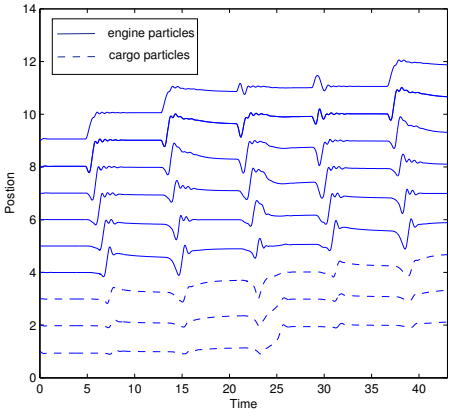

Fig. 4. Directed motion with cargo.

$$
\begin{aligned}
\dot{x}_{22} &= -(1/m)\{\eta x_{22} + \frac{2\pi}{b}\Phi_0 \sin(2\pi x_{21}/b) \\
&\quad +k(|x_{21}-x_{11}|-a) \\
&\quad -k(|x_{31}-x_{21}|-a)\} \qquad (12)\\
\dot{x}_{31} &= x_{32} \qquad (13)\\
\dot{x}_{32} &= -(1/m)\{\eta x_{32} + \frac{2\pi}{b}\Phi_0 \sin(2\pi x_{31}/b) \\
&\quad +k(|x_{31}-x_{21}|-a) - k(|x_{41}-x_{31}|-a)\} \\
\dot{x}_{41} &= x_{42} \qquad (14)\\
\dot{x}_{42} &= -(1/m)\{\eta x_{42} + \frac{2\pi}{b}\Phi_0 \sin(2\pi x_{41}/b) \\
&\quad +k(|x_{41}-x_{31}|-a) \\
&\quad -k[|x_{51}-x_{41}|-a(1+\alpha(4qb+\omega t))]\} \qquad (15)\\
\dot{x}_{i1} &= x_{i2} \qquad (16)\\
\dot{x}_{i2} &= -(1/m)\{\eta x_{i2} + \frac{2\pi}{b}\Phi_0 \sin(2\pi x_{i1}/b) \\
&\quad +k[|x_{i1}-x_{i-1,1}|-a(1+\alpha((i-1)qb+\omega t))] \\
&\quad -k[|x_{i+1,1}-x_{i1}|-a(1+\alpha(iqb+\omega t))]\} \qquad (17)\\
&\quad i=5,\ldots,8, \\
\dot{x}_{91} &= x_{92} \qquad (18)\\
\dot{x}_{92} &= -(1/m)\{\eta x_{92} + \frac{2\pi}{b}\Phi_0 \sin(2\pi x_{91}/b) \\
&\quad +k[|x_{91}-x_{81}|-a(1+\alpha(8qb+\omega t))]\} \qquad (19)
\end{aligned}
$$

where particles $i = 1, 2, 3$ are cargo particles, and $i = 4, \ldots, 10$ are engine particles.

Fig. 4 shows the directed motion of the coupled particle chain with cargo.

Although numerical simulations clearly demonstrate that the atomic scale engine model (1) is capable of transportation functionalities, analytic understanding of the nonlinear model and its complex dynamics is missing. This paper presents results in explaining the dynamic behavior of the model analytically using control theoretical methods. We focus on the step motion shown in Section II-A in this paper.

III. Stability Analysis of a 3-Particle Chain

In this section, we analyze the stability of the equilibrium points of the 3-particle chain as shown in (6), and verify that the equilibrium points shown in Fig. 2 are locally stable. For this purpose, we neglect the sinusoidal term in the function $\alpha(s)$ of (5) as it provides a temporary perturbation. Due to physical constraints of the 3-particle system, we have $x_{i+1,1} > x_{i1} > x_{i-1,1}$. Equation (6) turns to

$$
\begin{aligned}
\dot{x}_{11} &= x_{12} \\
\dot{x}_{12} &= -\frac{\eta}{m}x_{12} - \frac{2\pi\Phi_0}{mb}\sin\frac{2\pi x_{11}}{b} \\
&\quad -\frac{k}{m}(x_{21}-x_{11}-a) \\
\dot{x}_{21} &= x_{22} \\
\dot{x}_{22} &= -\frac{\eta}{m}x_{22} - \frac{2\pi\Phi_0}{mb}\sin\frac{2\pi x_{21}}{b} \\
&\quad -\frac{k}{m}(x_{31}-2x_{21}+x_{11}) \\
\dot{x}_{31} &= x_{32} \\
\dot{x}_{32} &= -\frac{\eta}{m}x_{32} - \frac{2\pi\Phi_0}{mb}\sin\frac{2\pi x_{31}}{b} \\
&\quad +\frac{k}{m}(x_{31}+x_{21}-a) \qquad (20)
\end{aligned}
$$

The equilibrium points of the couple particles are at $(x^*_{i1}, 0)$ where $x^*_{i1}, i = 1, 2, 3$, are solutions to the following algebraic equations:

$$
\begin{aligned}
\frac{2\pi\Phi_0}{mb}\sin\frac{2\pi x^*_{11}}{b} + \frac{k}{m}(x^*_{21}-x^*_{11}-a) &= 0, \\
\frac{2\pi\Phi_0}{mb}\sin\frac{2\pi x^*_{21}}{b} + \frac{k}{m}(x^*_{31}-2x^*_{21}+x^*_{11}) &= 0, \\
\frac{2\pi\Phi_0}{mb}\sin\frac{2\pi x^*_{31}}{b} - \frac{k}{m}(x^*_{31}-x^*_{21}-a) &= 0.
\end{aligned} \qquad (21)
$$

Define new states as $z_{i1} = x_{i1} - x^*_{i1}, z_{i2} = x_{i2}$, and linearize it around its equilibrium. We obtain

$$
\begin{aligned}
\dot{z}_{i1} &= z_{i2} \\
\dot{z}_{i2} &= -\rho\cos\left(\frac{2\pi}{b}x^*_{i1}\right)z_{i1} - \gamma z_{i2} \\
&\quad +\kappa(z_{i+1,1}-2z_{i1}+z_{i-1,1}) \\
&\quad -\varepsilon\sin x^*_{i1} + \kappa(x^*_{i+1,1}-2x^*_{i1}+x^*_{i-1,1}) \\
&= -\rho\cos\left(\frac{2\pi}{b}x^*_{i1}\right)z_{i1} - \gamma z_{i2} \\
&\quad +\kappa(z_{i+1,1}-2z_{i1}+z_{i-1,1}) \qquad (22)
\end{aligned}
$$

where we denote $\varepsilon = \frac{2\pi\Phi_0}{mb}, \rho = \varepsilon * 2\pi/b, \gamma = \frac{\eta}{m}, \kappa = \frac{k}{m}$. Note that the last equal sign holds due to the equilibrium equation (21). Note also that $\rho = \kappa$ for the parameters chosen in (7).

Stacking the state space equations for $i = 1, 2, \ldots, N$, we obtain

$$
\dot{z} = \overline{A}z + \overline{B}\,\overline{Q}z \qquad (23)
$$

where $z = [z_{11},\ z_{12},\ z_{21}\ z_{22},\ z_{31},\ z_{32}]^T$,

$$
\overline{A} = I_3 \otimes A, \quad \overline{B} = I_3 \otimes B, \quad \overline{Q} = Q \otimes \begin{bmatrix} 1 & 0 \end{bmatrix}, \qquad (24)
$$

and

$$A = \begin{bmatrix} 0 & 1 \\ 0 & -\gamma \end{bmatrix}, \qquad B = \begin{bmatrix} 0 \\ 1 \end{bmatrix}, \tag{25}$$

Q is represented in (26), and I_3 is the identity matrix of order 2. Here $\otimes$ denotes the Kronecker product.

To analyze the stability of the system (24), we need to decouple the interactions between particle subsystems. To achieve it, we define a similarity transformation $z = \overline{T}\zeta$ ([19]). In the new coordinate, the system dynamics is

$$\dot{\zeta} = H\zeta. \tag{27}$$

We show how to choose $\overline{T}$ and present H accordingly.

Since Q is a real symmetric matrix, according to Lemma 1 in the Appendix, there exists a unitary matrix T such that $T^{-1}QT = D$ where D is a diagonal matrix of eigenvalues of Q. Let

$$\overline{T} = T \otimes I_2 \tag{28}$$

where I_2 is the 2×2 identity matrix. Then:

$$\begin{aligned} H &= \overline{T}^{-1}(\overline{A} + \overline{B}\,\overline{Q})\overline{T} \\ &= \overline{T}^{-1}\left[I_3 \otimes A + (I_3 \otimes B)(Q \otimes \begin{bmatrix} 1 & 0 \end{bmatrix})\right]\overline{T} \\ &= \overline{T}^{-1}\left(I_3 \otimes A + Q \otimes \begin{bmatrix} 0 & 0 \\ 1 & 0 \end{bmatrix}\right)\overline{T} \\ &= \left(T^{-1}I_3T\right) \otimes A + \left(T^{-1}QT\right) \otimes \begin{bmatrix} 0 & 0 \\ 1 & 0 \end{bmatrix} \\ &= I_3 \otimes A + D \otimes \begin{bmatrix} 0 & 0 \\ 1 & 0 \end{bmatrix} \end{aligned} \tag{29}$$

We can see that H is block diagonal, and the block diagonal element of H writes:

$$H_{ii} = \begin{bmatrix} 0 & 1 \\ \beta_i & -\gamma \end{bmatrix}, \tag{30}$$

where $\beta_i, i = 1, 2, \ldots, N$ are eigenvalues of Q. The stability of the system depends on the sign of the real parts of $\beta_i, i = 1, 2, 3$:

1) If $\beta_i, i = 1, 2, 3$ have negative real parts, the eigenvalues of $H_{ii}, i = 1, 2, 3$ have also negative real parts, and so does the matrix H. This indicates that the system is asymptotically stable at these points. Due to the similarity transformation, the same stability result holds for the original system $\dot{z} = (\overline{A} + \overline{B}\,\overline{Q})z$. Furthermore, local stability of the original nonlinear system (20) can be deduced from the stability analysis of its linearized system (23) ([20], Theorem 3.1).
2) If β_i has a positive real part for any $i \in [1, 3]$, eigenvalues of $H_{ii}, i = 1, 2, 3$, also have positive real parts. With the same arguments as above, the system (20) is unstable at these points.

Checking the structure of matrix Q in (26), we have the following cases:

- If $\cos\left(\frac{2\pi}{b}x^*_{i1}\right) \geq 0$ for all i with strict inequality for at least one i, the matrix $-Q$ is an M-matrix and $\beta_i < 0$ for all i, according to Lemma 2. Therefore, Q is Hurwitz and the system is asymptotically stable;
- If $\cos\left(\frac{2\pi}{b}x^*_{i1}\right) = 0$ for all i, Q has one (and only one) eigenvalue 0 according to Lemma 3. The linear system (23) is marginally stable and the stability of the nonlinear system (20) could be either stable or unstable;
- If $\cos\left(\frac{2\pi}{b}x^*_{i1}\right) \leq 0$ for all i with strict inequality for at least one i, we can represent Q as in (31). Since Φ in (31) is an irreducible and non-negative matrix, it has a positive eigenvalue, r, equal to the spectral radius of Φ, which is between $2k + \min\{-\cos\left(\frac{2\pi}{b}x^*_{11}\right), \ldots, -\cos x^*_{N1}\}$ and $2k + \max\{-\cos\left(\frac{2\pi}{b}x^*_{11}\right), \ldots, -\cos x^*_{N1}\}$ ([21], page 537). Therefore, Q has at least one positive eigenvalue. The system is unstable;
- If $\cos\left(\frac{2\pi}{b}x^*_{i1}\right), i = 1, 2, 3$, have mixed signs, the system could be either stable or unstable and numerical calculations is necessary to determine the sign of the real parts of the eigenvalues of Q.

We have the following theorem whose proof follows directly from the above analysis due to similarity transformation defined in (28). (One can also refer to the proof of Theorem 1 in [19] for a similar idea.)

Theorem 1: The equilibrium point $(x^*_{11}, 0, x^*_{21}, 0, x^*_{31}, 0)$ of the system (20) is locally asymptotically stable if $\cos\left(\frac{2\pi}{b}x^*_{i1}\right) \geq 0$ for all $i = 1, 2, 3$ with strict inequality for at least one i, and it is unstable if $\cos\left(\frac{2\pi}{b}x^*_{i1}\right) \leq 0$ for all $i = 1, 2, 3$ with strict inequality for at least one i.

From the above theorem, we have the following corollary.

Corollary 1: For the set of parameters chosen in (7), the equilibrium point $(x^*_{11}, 0, x^*_{21}, 0, x^*_{31}, 0)$ of the system (20) with $x^*_{i1}, i = 1, 2, 3$, represented in the following:

$$\begin{aligned} x^*_{11} &= (l-1)b - d, \\ x^*_{21} &= lb, \\ x^*_{31} &= (l+1)b + d, \end{aligned} \tag{32}$$

where $l = 0, \pm 1, \pm 2, \ldots,$ and $0 < d < b$, are locally asymptotically stable; and the equilibrium point represented by

$$\begin{aligned} x^*_{11} &= (l-1)b + \frac{b}{2} - d, \\ x^*_{21} &= lb + \frac{b}{2}, \\ x^*_{31} &= (l+1)b + \frac{b}{2} + d, \end{aligned} \tag{33}$$

where $l = 0, \pm 1, \pm 2, \ldots,$ and $0 < d < \frac{b}{2}$, are unstable.

Proof: For the set of equilibrium points (32) and (33), we can see that both of them satisfy the equilibrium equation (21). For the set of parameters chosen in (7), we have further calculated that $d = 0.0504$ for both the equilibrium points represented in (32) and (33). We can then apply Theorem 1 to obtain the stability. We have the following two cases:

- For the equilibrium point represented in (32), we have

$$\begin{aligned} \cos\left(\frac{2\pi}{b}x^*_{11}\right) &= \cos\left(\frac{2\pi((l-1)b-d)}{b}\right) \\ &= \cos(2\pi * 0.0504) > 0 \end{aligned}$$

$$Q = \begin{bmatrix} -\kappa - \rho\cos\left(\frac{2\pi}{b}x_{11}^*\right) & \kappa & 0 \\ \kappa & -2\kappa - \rho\cos\left(\frac{2\pi}{b}x_{21}^*\right) & \kappa \\ 0 & \kappa & -\kappa - \rho\cos\left(\frac{2\pi}{b}x_{31}^*\right) \end{bmatrix}. \quad (26)$$

$$Q = \begin{bmatrix} \kappa - \rho\cos\left(\frac{2\pi}{b}x_{11}^*\right) & \kappa & 0 \\ \kappa & -\rho\cos\left(\frac{2\pi}{b}x_{21}^*\right) & \kappa \\ 0 & \kappa & \kappa - \rho\cos\left(\frac{2\pi}{b}x_{31}^*\right) \end{bmatrix} + (-2\kappa)I_3 \stackrel{def}{=} \Phi + (-2\kappa)I_3. \quad (31)$$

$$\begin{aligned} \cos\left(\frac{2\pi}{b}x_{21}^*\right) &= \cos\left(\frac{2\pi(lb)}{b}\right) \\ &= \cos(2l\pi) > 0 \\ \cos\left(\frac{2\pi}{b}x_{31}^*\right) &= \cos\left(\frac{2\pi((l+1)b+d)}{b}\right) \\ &= \cos(2\pi * 0.0504) > 0 \end{aligned}$$

Therefore, this equilibrium is asymptotically stable according to Theorem 1;

- For the equilibrium point represented in (32), we have

$$\begin{aligned} \cos\left(\frac{2\pi}{b}x_{11}^*\right) &= \cos\left(\frac{2\pi((l-1)b+b/2-d)}{b}\right) \\ &= \cos(\pi - 2\pi * 0.0504) < 0 \\ \cos\left(\frac{2\pi}{b}x_{21}^*\right) &= \cos\left(\frac{2\pi(lb+b/2)}{b}\right) \\ &= \cos(2l\pi + \pi) < 0 \\ \cos\left(\frac{2\pi}{b}x_{31}^*\right) &= \cos\left(\frac{2\pi((l+1)b+b/2+d)}{b}\right) \\ &= \cos(\pi + 2\pi * 0.0504) < 0 \end{aligned}$$

Therefore, this equilibrium is unstable according to Theorem 1.

Remark 1: From Corollary 1, the stability of the system (20) is similar to that of the well-known pendulum system, where stable and unstable equilibrium points arise in an alternating sequence in the upward $2l\pi$ and the downward $(2l+1)\pi$ positions. Note that our system (20) has a period of b, and the equilibrium points around lb are stable, while $(lb + \frac{b}{2})$ are not. Therefore, if the perturbation term $\alpha(\cdot)$ defined in (4) is big enough to move the system to the neighborhood of the next stable equilibrium, the system will stay there and generate a step motion. This explains what we observe in Fig. 2, and we verify that the system moves from the position $[x_{11}, x_{21}, x_{31}] = [1, 2, 3]$ to $[x_{11}, x_{21}, x_{31}] = [1.9496, 3, 4.0504]$, since the latter is a stable equilibrium satisfying (32) with $l = 3$.

Remark 2: The system may have other equilibrium points besides those represented in (32) and (33). Stability of other equilibrium points can be determined using Theorem 1.

To further verify the stability results claimed in Corollary 1, we performed more simulations in Matlab. Fig. 5 shows that stability of (32) with $l = 10$ and $l = -1$. For the unstable equilibrium (33), we show in Fig. 6 that the system may move to the stable equilibrium either before or after the current equilibrium, similar to the unstable (saddle) point at the $((2l+1)\pi)$ position in the pendulum system. Note that the initial conditions are chosen randomly around the interested equilibrium in the simulations.

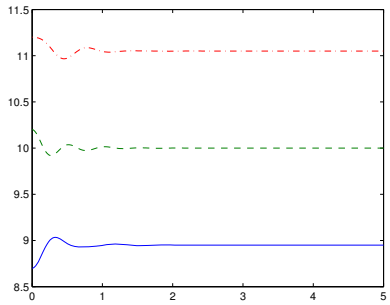

(a)

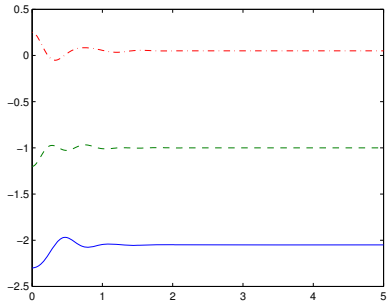

(b)

Fig. 5. Local stability of equilibrium (32) with (a) $l = 10$, and (b) $l = -1$.

IV. Conclusions

In this paper, we first re-considered an atomic scale engine model that is composed of a one-dimensional coupled particles [1]. We then showed numerically that the model exhibits directed motions under asymmetric particle coupling, which include a step motion, continuous moving, and carrying cargo loads. In order to explain analytically why directed motion happens, we studied the stability of the model with 3 coupled particles. Using control theoretical methods, we proved that stable and unstable equilibrium points arise in an alternating sequence thus step motion can be deduced by perturbations. Matlab simulations verified our analytic results. Future work includes further investigation of the continuous motion and cargo carrying behaviors as well as how to choose control parameters for different motion types.

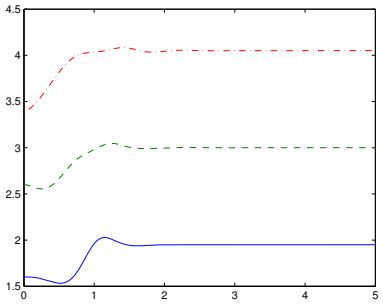

(a)

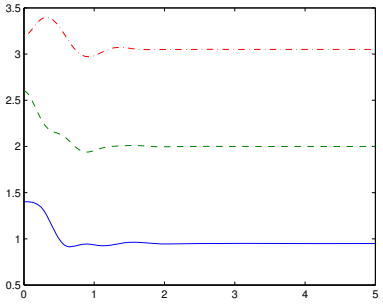

(b)

Fig. 6. Local unstability of equilibrium (33) with $l = 2$.

V. ACKNOWLEDGMENTS

This work was supported in part by the National Science Foundation under Grants CMMI#0825613 and DUE#0837584.

APPENDIX

Lemma 1 ([22], page 171): Spectral Theorem for Symmetric Matrices: If A is an $n \times n$ real symmetric matrix, then there always exist matrices L and D such that $L^T L = LL^T = I$ and $LAL^T = D$, where D is the diagonal matrix of eigenvalues of A.

Lemma 2 ([21]): Let $A = [a_{ij}]_{i,j=1}^n \in \Re^{n\times n}$ and assume that $a_{ii} > 0$ for each i and $a_{ij} \leq 0$ whenever $i \neq j$. If A is diagonally dominant, that is,

$$a_{ii} > \sum_{j=1, j\neq i}^{n} |a_{ij}|, \quad i = 1, 2, \ldots, n,$$

or, if A is irreducible and

$$a_{ii} \geq \sum_{j=1, j\neq i}^{n} |a_{ij}|, \quad i = 1, 2, \ldots, n,$$

with strict inequality for at least one i, then A is an M-matrix. A symmetric M-matrix is positive definite.

Lemma 3 ([23], Appendix A): Define the set W consisting of all zero row sum matrices which have only nonpositive off-diagonal elements. A matrix $A \in W$ satisfies:

1) All eigenvalues of A are nonnegative;
2) 0 is an eigenvalue of A;
3) 0 is an eigenvalue of multiplicity 1 if A is irreducible.

REFERENCES

[1] M. Porto, M. Urbakh, and J. Klafter. Atomic scale engines: Cars and wheels. *Physical Review Letters*, 84(26):6058–6061, 2000.
[2] R. P. Feynman, R. Leighton, and M. Sands. *The Feynman Lectures in Physics*. Addison-Wesley, Reading, MA, 1963.
[3] M. O. Magnasco. Forced thermal ratchets. *Physical Review Letters*, 71(10):1477–1481, 1993.
[4] P. Reimann. Supersymmetric ratchets. *Physical Review Letters*, 86:4992–4995, 2001.
[5] B. J. Gabrys, K. Pesz, and S. J. Bartkiewicz. Brownian motion, molecular motors and ratchets. *Physica A*, 336:112–122, 2004.
[6] A. Huxley and J. Howard. How molecular motors work in muscle. *Nature*, 391:239–240, 1998.
[7] F. Julicher, A.Ajdari, and J. Prost. Modeling molecular motors. *Reviews of Modern Physics*, 69(4):1269–1281, 1997.
[8] T. R. Kelly, H. D. Silva, and R. A.Silva. Unidirectional rotary motion in a molecular system. *Nature*, 401:150–152, 1999.
[9] N. Koumura, R. W. J. Zijlstra, R. A.van Delden, N. Harada, and B.L. Feringa. Light-driven monodirectional molecular rotor. *Nature*, 401:152–155, 1999.
[10] J. A. Tuszynski and M. Kurzynski. *Introduction to Molecular Biophysics*. CRC Press, Boca Raton, 2003.
[11] Y. Shirai, J.F. Morin, T. Sasaki, J. M. Guerrero, and J.M. Tour. Recent progress on nanovehicles. *Chemical Society Reviews*, 35:1043–1055, 2006.
[12] Y. Shirai, A. J. Osgood, Y. Zhao, K. F. Kelly, and J. M. Tour. Directional control in thermally driven single-molecule nanocars. *Nano Letters*, 5(11):2330–2334, 2005.
[13] Y. F. Gao and Z. Suo. Guided self-assembly of molecular dipoles on a substrate surface. *Journal of Applied Physics*, 93:4276–4282, 2003.
[14] Z. Suo and W. Hong. Programmable motion and patterning of molecules on solid surfaces. *Proceedings of the National Academy of Sciences of the United States*, 101(21):7874–7879, 2004.
[15] Z. Suo. The molecular car and its on-chip infrastructure. MIT ME seminar, http://www.seas.harvard.edu/suo/index.html, 2003.
[16] M. Porto. Atomic scale engines: Taking a turn. *Acta Physica Polonica B*, 32(2):295–306, 2001.
[17] M. Porto, M. Urbakh, and J. Klafter. Molecular motor that never steps backwards. *Physical Review Letters*, 85(3):491–494, 2000.
[18] V. L. Popov. Nanomachines: a general approach to inducing a directed motion at the atomic level. *International Journal of Non-Linear Mechanics*, 39:619–633, 2004.
[19] Y. Guo and Z. Qu. Control of frictional dynamics of a one-dimensional particle array. *Automatica*, 44:2560–2569, 2008.
[20] J. J. E. Slotine and W. Li. *Applied Nonlinear Control*. Prentics Hall, New Jersey, 1991.
[21] P. Lancaster and M. Tismenetsky. *The Theory of Matrices with Applications*. Academic Press, second edition, 1985.
[22] C. Godsil and G. Royle. *Algebraic Graph Theory*. Springer, New York, 2001.
[23] C. W. Wu. *Synchronization in Coupled Chaotic Circuits and Systems*. World Scientific, Singapore, 2002.